Photoluminescence of electron-irradiated 4*H*-SiC

T. Egilsson*
Department of Physics and Measurement Technology, Linköping University, S-581 83 Linköping, Sweden

A. Henry
Department of Physics and Measurement Technology, Linköping University, S-581 83 Linköping, Sweden and ABB Corporate Research, S-721 78 Västerås, Sweden

I. G. Ivanov
Department of Physics and Measurement Technology, Linköping University, S-581 83 Linköping, Sweden

J. L. Lindström
Department of Physics and Measurement Technology, Linköping University, S-581 83 Linköping, Sweden and National Defence Research Institute, P.O. Box 1165, S-581 11 Linköping, Sweden

E. Janzén
Department of Physics and Measurement Technology, Linköping University, S-581 83 Linköping, Sweden
(Received 26 June 1998; revised manuscript received 9 December 1998)

We report the properties of a photoluminescence (PL) spectrum, here called E_A, appearing after room-temperature electron irradiation of 4*H*-SiC. The spectrum consists of several sharp no-phonon lines accompanied by a broad phonon-assisted structure. Among the samples investigated were epitaxial layers of low residual doping and highly doped substrates. Annealing at around 750 °C induces an abrupt change in the spectrum. Further annealing steps occur at temperatures above 750 °C eventually leading to the dominance of the strong D_{I} PL spectrum. We have investigated the polarization, temperature dependence, and excitation properties of the E_A PL. Up to 40 no-phonon lines can be resolved in the E_A spectrum. All the no-phonon lines appear within the span of approximately 100 meV (2.8–2.9 eV). By photoluminescence excitation spectroscopy we are able to establish the relationship between most of the different lines. The lines come in groups of two to four lines. The general characteristics of the line groups suggest that they are due to bound exciton recombination at isoelectronic defect centers. [S0163-1829(99)08611-7]

I. INTRODUCTION

The material properties of silicon carbide (SiC) semiconductors make them well suited for high-power, high-temperature, and high-frequency electronics. SiC has a wider band gap, higher thermal conductivity, higher breakdown electric field strength, and greater thermal and chemical stability than silicon (Si), the semiconductor that is currently used for most power electronic devices. However, the growth and device processing technology of SiC is still immature and needs to be improved if SiC is to replace Si. SiC exists in several different polytypes of which the 3*C*, 4*H*, 6*H*, and 15*R* polytypes are the most common. Of these, the 4*H* polytype is considered to be the most appropriate for high-power applications, as it has the widest band gap and an almost isotropic electron mobility.

Several common semiconductor device processing steps involve some type of irradiation. For SiC, doping by ion implantation is of particular importance since diffusion doping is only possible at very high temperatures (>1800 °C).[1] In the processing of Si power electronic devices, it is common to use neutron transmutation for *n*-type doping of large areas and electron irradiation for lifetime control. These techniques are also likely to play a role in future SiC technology. Irradiation creates defects in the material. These are used to an advantage in lifetime control, but most often they are unwanted by-products. It is important from a technological point of view to study these defects and their influence on the material characteristics. Another reason for studying irradiation-induced defects is their fundamental nature. Irradiation by high-energy particles produces primary defects such as single vacancies and interstitials. In contrast to Si, some of the primary defects seem to be stable at room temperature in SiC. The main evidence for this is the observation of the silicon and carbon monovacancies (V_{Si},V_{C}) by electron paramagnetic resonance (EPR) in SiC irradiated at room temperature.[2–5]

Studies of photoluminescence (PL) in SiC related to radiation damage have mainly focused in the past on strong emissions persisting after high-temperature annealing such as the well-known D_{I} and D_{II} PL bands.[6,7] In the case of heavy particle bombardment, the damage is often so severe directly after irradiation that annealing is needed to be able to see PL from the samples. Electron irradiation (EI) creates much less concentrated damage, and PL can therefore usually be observed without any annealing.[8–11] In Fig. 1 we show a diagram indicating the energy ranges where most of the PL emissions occur in 4*H*-SiC after EI at room temperature. In the left side of the figure we show the situation directly after EI, and on the right side after high-temperature

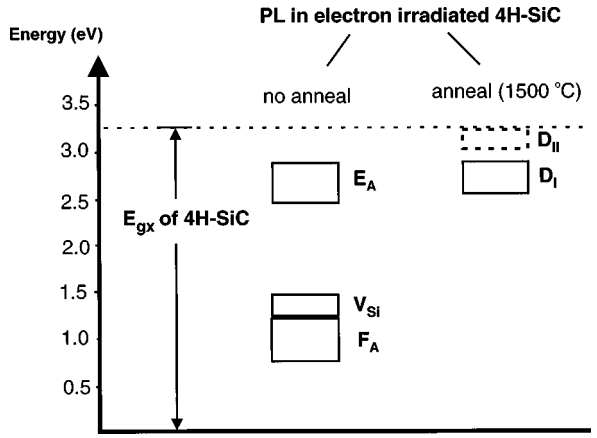

FIG. 1. The figure shows the energy ranges of the main PL spectra induced by room-temperature electron irradiation of 4*H*-SiC. The excitonic band-gap energy of 4*H*-SiC is shown for comparison. The left side of the figure shows the situation directly after electron irradiation, whereas the right side shows the bands that are dominant after high-temperature annealing (~1500 °C).

annealing (~1500 °C). The D_{II} band is enclosed by dotted lines in the figure because we do not observe it in our EI material. It is, however, commonly observed after ion or neutron bombardment. It has been proposed that the D_{II} band is caused by carbon di-interstitials,[6,7] so its absence in EI material may be due to the relatively low defect density. To our knowledge, the PL spectra observed in the highest and lowest energy regions directly after EI have not previously been given names. Thus, for the sake of convenience we will refer to them here as the E_A and F_A spectra, respectively.

The D_I band is observed in all the common SiC polytypes and its energy shifts with the band-gap energy. The same applies for the E_A spectrum. The energy of the V_{Si} band, on the other hand, is about the same in 4*H*- and 6*H*-SiC in spite of the band-gap difference,[12] but has not been observed in the smaller band-gap polytype 3*C*-SiC. The energies of the main lines in the F_A spectrum are also very similar in 4*H*- and 6*H*-SiC.[11,13] In 3*C*-SiC, PL in the F_A region is also observed,[14] but its properties are different from the case of the 4*H* and 6*H* polytypes. A detailed study has recently been conducted on the V_{Si} band in both 4*H*- and 6*H*-SiC.[12,15,16] The number of no-phonon lines in this band is equal to the number of inequivalent substitutional sites (that is, two in 4*H* and three in 6*H*). From the hyperfine splitting observed in optically detected magnetic resonance (ODMR) spectra it was concluded that the lines were related to single Si vacancies (V_{Si}). The PL lines are believed to be caused by internal transitions. The band was found to anneal out at approximately 750 °C, similar to the V_{Si} EPR signals.[2,3,5] The E_A and F_A spectra consist of several no-phonon lines and their associated phonon replicas. In contrast to the V_{Si} band these remain for the most part unidentified both regarding the nature of the transitions and the responsible defects.

In this paper we report a study of the properties of the E_A PL spectrum in electron-irradiated 4*H*-SiC. Annealing below 750 °C induces only minor changes in the PL spectrum. However, at higher annealing temperatures it transforms in a number of abrupt steps until the D_I spectrum dominates. We have investigated the polarization, temperature dependence, and excitation properties of the E_A PL. A preliminary investigation of the dependence on irradiation dose and doping was also carried out. Up to 40 no-phonon lines can be resolved in the E_A spectrum. All the no-phonon lines appear within the span of approximately 100 meV (2.8–2.9 eV). An essential part of our work has been to sort out this complicated spectrum by establishing the relationship between the different lines. This has been accomplished by means of photoluminescence excitation (PLE) spectroscopy and selective excitation. As it turns out, the lines come in groups of two to four lines. The relative PL intensities of the lines within each line group depend on measurement temperature and reflect their different oscillator strengths as well as the different energies. The general characteristics of the line groups suggest that they are due to bound exciton recombination at isoelectronic defect centers.

The paper is organized as follows: (i) In Sec. II we describe the samples and experimental details; (ii) Sec. III A presents the E_A PL spectrum in 4*H*-SiC and its temperature dependence. The effect of post annealing and initial doping are also discussed; (iii) in Sec. III B the PLE results are presented; (iv) Sec. III C deals with the phonon structure; (v) in Sec. IV we discuss the results and their implications; (vi) finally, in Sec. V we give a summary.

II. EXPERIMENT

Several different types of 4*H*-SiC samples were investigated. Among these were n^+- and p^+-type substrates and epilayers grown by chemical vapor deposition (CVD) with different levels of *n*- or *p*-type residual doping. The samples were [0001] oriented with off-axis cuts of 8°. The samples were irradiated at room temperature with 2 MeV electrons in doses varying between 10^{15} and $10^{18}\,cm^{-2}$. The damage caused by the electron irradiation is expected to be approximately uniform throughout the entire thickness of the samples.

For the optical experiments, He bath cryostats with facilities for temperature variation were used. We used the 334.5 nm uv line of an Ar^+ ion laser for above band-gap excitation of the PL spectra. For the PLE and the selective PL (SPL) measurements, we used blue light from a dye laser pumped with the multiline uv output of an Ar^+ ion laser. For the PLE and SPL the luminescence was spectrally resolved by a 0.85 m SPEX 1404 double grating monochromator fitted with 1800 grooves/mm gratings, and detected by a Hamamatsu photomultiplier tube (PMT) operating in photon-counting mode. The normal PL spectra were recorded either with the above system or a liquid-nitrogen-cooled CCD camera attached to a single JY HR460 monochromator fitted with a 2400 grooves/mm grating.

Most of the PL measurements were carried out in a near-backscattering (NBS) configuration. However, as the crystal *c* axis of our samples is close to being perpendicular to the surface, this configuration only gives access to the $\overline{E} \perp \overline{c}$ component of the PL.[17] Therefore, to determine the polarization of the different PL lines we also measured the PL through a cleaved edge while exciting through the surface. This configuration allows the selection of either the $\overline{E} \perp \overline{c}$ and $\overline{E} \parallel \overline{c}$ component by a polarizer. PL contribution from the sur-

face region was avoided by placing a barrier of silver-paste close to the sample edge. The spectra were corrected for the polarization effect of the monochromator. All the PL spectra shown in this paper except those in Fig. 4 were measured in the NBS configuration.

The PLE spectra were recorded by monitoring the PL at certain no-phonon line positions (or at their phonon replicas) while scanning the dye laser excitation above (or across) the relevant no-phonon line. SPL spectra were taken by adjusting the dye laser excitation wavelength to one of the PLE peaks and then recording the PL. For both PLE and SPL, a NBS configuration was used.

III. RESULTS

A. The E_A photoluminescence spectrum

Before irradiation, the PL spectrum in most of the samples was dominated by the near-band-gap free and nitrogen bound exciton lines. After irradiation this PL was weak, but instead several sharp PL lines had appeared in the region 4250–4500 Å followed by a broad structure extending to about 5500 Å. This is the E_A PL spectrum. Most of the sharp lines are no-phonon lines, whereas the broad part is due to phonon-assisted transitions. The linewidths of the E_A no-phonon lines are typically around 0.6 Å (0.4 meV) in our samples.

The E_A PL spectrum consisted of the same lines in all the investigated 4*H*-SiC samples. However, the relative intensity of lines was not always the same. The quality of the E_A spectrum in terms of linewidth and signal strength was highest in epilayers of low residual doping. Most of the results presented in this paper are based on measurements on a 40 μm thick CVD layer with *n*-type residual doping in the low $10^{14}\,\mathrm{cm}^{-3}$ range, grown on an n^+ [0001] oriented substrate with an off-axis cut of 8°, and irradiated with 2 MeV electrons at a dose of $10^{17}\,\mathrm{cm}^{-2}$. The sample will be referred to in the following as sample *A*.

In Fig. 2 we show the effect of annealing on the no-phonon part of the PL spectrum of sample *A*. The spectra were taken at 15 K. Annealing at temperatures below 750 °C has little effect on the spectrum. However, when the sample is annealed at 750 °C for 30 min, a drastic change occurs [see Fig. 2(b)]. The strong lines in the spectral region between 4330 and 4370 Å disappear completely, while many of the lines at higher energies (shorter wavelengths) are enhanced. The D_{I} lines L_1 and M_1 that are barely visible before annealing are now strong. After annealing at 1500 °C for 30 min [see Fig. 2(c)] only the D_{I} PL can be observed.[18]

The effect of initial doping and irradiation dose on the E_A spectrum was not investigated thoroughly, but the main trends were established. For irradiation doses in the range 10^{15}–$10^{17}\,\mathrm{cm}^{-2}$, the E_A PL spectrum is similar for all types of samples irrespective of their doping. The intensity of the spectrum is highest in the lowest doped samples and increases with the dose. On the other hand, when the dose is increased from 10^{17} to $10^{18}\,\mathrm{cm}^{-2}$, the intensity of the spectrum decreases and in the case of highly doped samples the relative intensities of the lines also change. Figure 3 shows the E_A spectrum for an n^- ($1\times10^{15}\,\mathrm{cm}^{-3}$) undoped CVD layer, an n^+ ($1\times10^{18}\,\mathrm{cm}^{-3}$) nitrogen-doped substrate, and a p^+ ($5\times10^{17}\,\mathrm{cm}^{-3}$) aluminum-doped substrate. The samples

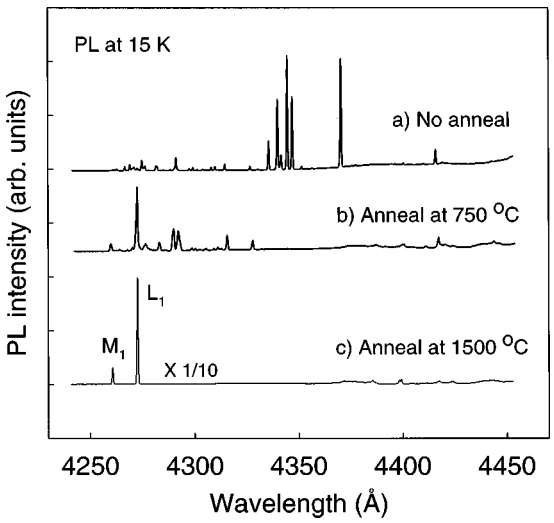

FIG. 2. The effect of annealing on the no-phonon part of the PL spectrum of sample *A*. The spectra were taken at 15 K. Annealing at temperatures below 750 °C has little effect on the spectrum. The D_{I} lines L_1 and M_1 that dominate the spectrum after annealing at 1500 °C are about one order of magnitude more intense than the lines of the (a) and (b) spectra.

were irradiated with the highest dose of electrons: $1\times10^{18}\,\mathrm{cm}^{-2}$. The labeling of the lines in the E_A spectrum is explained in Sec. III B. Apart from being somewhat weaker, the E_A spectrum of the n^- sample is almost identical to the E_A spectrum of sample *A*. In the case of the n^+ and p^+ samples, on the other hand [Figs. 3(b) and 3(c)], only part of the E_A spectrum is sufficiently strong to be observed. In the spectrum of the p^+ sample, the b_1 no-phonon line dominates. The line b_1 (78 meV) is a phonon replica of the b_1 line, as will be shown in Sec. III C. In the spectrum of the n^+ sample, both the b_1 and f_1 lines are enhanced relative to the other no-phonon lines.

Figure 4 shows the polarization as well as the temperature dependence of the no-phonon lines in the E_A spectrum of

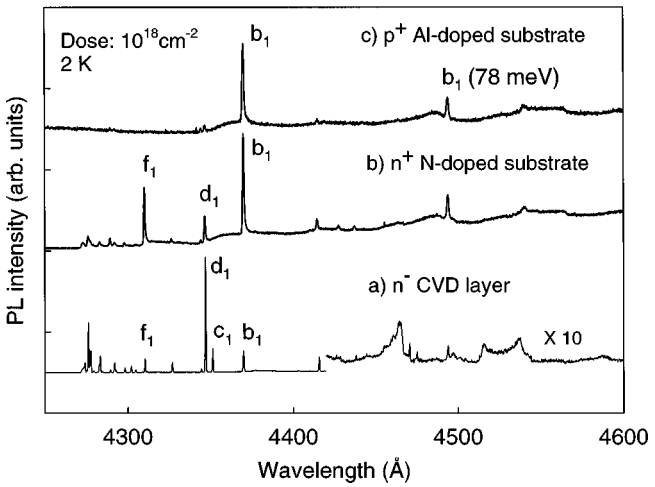

FIG. 3. The effect of doping on the E_A spectrum of 4*H*-SiC irradiated with a high dose ($1\times10^{18}\,\mathrm{cm}^{-3}$) of electrons. The figure shows the E_A spectra of (a) an n^- ($1\times10^{15}\,\mathrm{cm}^{-3}$) undoped CVD layer, (b) an n^+ ($1\times10^{18}\,\mathrm{cm}^{-3}$) nitrogen-doped substrate, and (c) a p^+ ($5\times10^{17}\,\mathrm{cm}^{-3}$) aluminum-doped substrate.

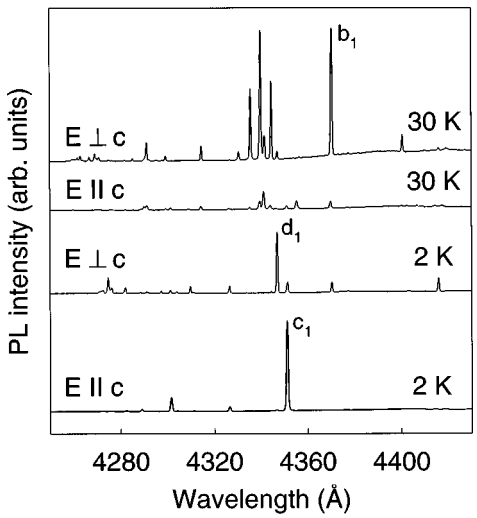

FIG. 4. Polarization as well as the temperature dependence of the E_A no-phonon lines in the PL spectrum of sample *A*. The lowest two PL spectra were taken at 2 K and show the $\overline{E}\|\overline{c}$ and $\overline{E}\perp\overline{c}$ components, respectively. The two uppermost spectra show the $\overline{E}\|\overline{c}$ and $\overline{E}\perp\overline{c}$ PL components at 30 K.

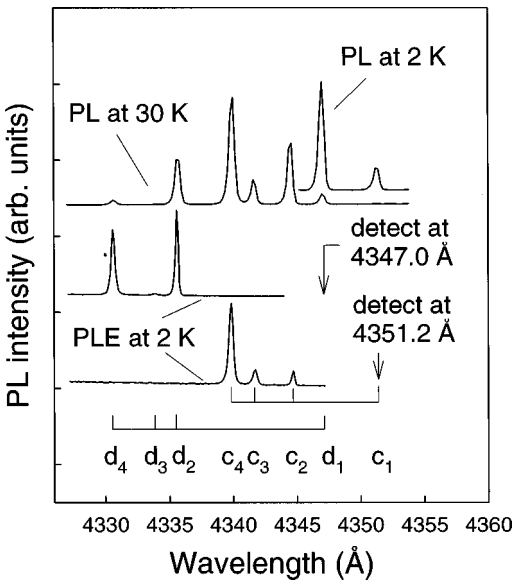

FIG. 5. PLE spectra at 2 K for the two low-temperature lines, c_1 and d_1, in the PL spectrum of sample *A* (see Fig. 4), and a comparison with PL spectra at 2 and 30 K.

sample *A*. The lowest two PL spectra were taken at 2 K and show the $\overline{E}\|\overline{c}$ and $\overline{E}\perp\overline{c}$ components, respectively. Due to scattering inside the material, the polarization of the lines is not perfect, so they can also be observed weakly in the spectrum of opposite polarization. The two uppermost spectra show the $\overline{E}\|\overline{c}$ and $\overline{E}\perp\overline{c}$ PL components at 30 K. Several new lines appear in the $\overline{E}\perp\overline{c}$ spectrum at 30 K, but at the same time many of the lines observable at 2 K disappear or become very weak. The $\overline{E}\|\overline{c}$ spectrum at 30 K consists mainly of the residual PL from the opposite polarization. From the spectra it can be seen that the main effect of increasing the temperature from 2 to 30 K is to shift the PL to lines at higher energies. Further increase of the temperature leads to broadening of the lines, and a slight shift to lower energies due to the lowering of the band gap. At temperatures above 100 K the the PL gradually quenches. The dependence on temperature is reminiscent of the D_{I} PL with its characteristic low- and high-temperature lines.[6,18] From the experience with the D_{I} PL, it is likely that each of the lines that can only be observed at low temperature is related to one or more of the high-temperature lines. In order to find the relationship between the low- and high-temperature lines of the E_A spectrum, we carried out PLE measurements. The results are described in the next section.

B. Photoluminescence excitation

Photoluminescence excitation spectroscopy proves to be a convenient way to sort out the complicated E_A spectrum. As an example, Fig. 5 shows the PLE spectra at 2 K for the two low-temperature lines, c_1 and d_1, in the spectrum of sample *A* (see Fig. 4), and a comparison with PL spectra at 2 and 30 K. When monitoring at the c_1 line position 4351.2 Å, and scanning the laser excitation towards lower wavelengths (higher energies), resonances appear at 4344.6, 4341.6, and 4340.0 Å (c_2, c_3, and c_4). These wavelengths correspond exactly to the positions of three of the high-temperature lines seen in the PL spectrum taken at 30 K. If we monitor instead at 4347 Å (d_1 line), resonances appear at 4335.6, 4334.2, and 4330.6 Å (d_2, d_3, and d_4). These resonances also correspond to high-temperature PL lines. This may be explained in the following way. Each of the centers responsible for the PL is associated with a group of excited energy states. Transitions from these states give rise to PL. The population of the different excited states is determined by the temperature. At 2 K only the lowest-energy states of each group have an appreciable population, and therefore only the lowest-energy PL lines (c_1 and d_1) are observed in the PL spectrum. At 30 K, the population of higher-energy states is no longer negligible and part of the PL therefore comes from transitions from those states. If the system is excited directly into a certain high-energy state at 2 K, it will rapidly relax to the lowest-energy state and give off PL from there. This explains the peaks observed in the PLE spectra. The fact that the c_1 and d_1 lines decrease in intensity with increasing temperature indicates that these transitions have lower oscillator strengths than the higher-energy transitions. Excitation into these states should therefore be less efficient than excitation into the higher-energy states. In the case of the d_1 line, this was confirmed by a separate PLE measurement on one of its phonon replicas. The spectrum contained the same PLE peaks as those shown in Fig. 5 but no peak was observed at the d_1 line position, showing that the associated transition has a very low oscillator strength.

In Fig. 6 we summarize our PLE results for the no-phonon lines of the E_A spectrum of sample *A*. Table I contains the positions of the lines labeled in the figure as well as their polarization and their dependence on measurement temperature. We were unable to carry out PLE measurements on the weakest lines in the E_A spectrum. The PLE spectra of 12 of the low-temperature no-phonon lines (indicated with dotted lines in the figure) were measured. In this way 12 groups of lines were established containing a total of 33 no-phonon lines. The total number of lines in the PL spectrum is about 40. All the groups of lines except the *b* group exhibit the

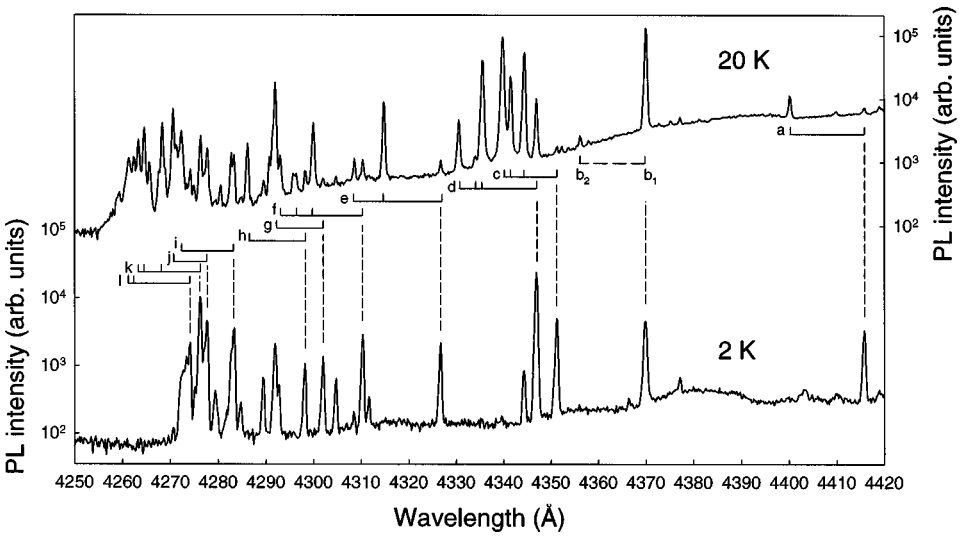

FIG. 6. The no-phonon part of the E_A PL spectrum of sample *A* at 2 and 20 K. Vertical dotted lines are placed above those PL lines for which we carried out PLE measurements. The grouping of lines, except for the two *b* lines, is based on the PLE results. The line groups are labeled in alphabetical order from right to left in the figure. Within each group the lines are numbered from right to left.

same general type of temperature behavior. There is one low-temperature line that decreases in intensity with increasing temperature, and one to three lines at higher energies that come up as the temperature increases. The PLE spectrum of the b_1 line did not contain any clear peaks. In spite of this, in Fig. 6 we have indicated by a dotted line a relation between the b_1 and b_2 lines. This is a tentative assignment based on the temperature and annealing dependence of the two lines. The absence of a peak at the b_2 line position in the PLE spectrum of the b_1 line does not contradict the assignment, since the b_2 line has $\overline{E}\|\overline{c}$ polarization whereas the excitation has $E\perp\overline{c}$ polarization.

C. Phonon structure

The phonon structure of the E_A spectrum is the superposition of the phonon replicas of all the different no-phonon lines. In order to see the phonon structure associated with one specific no-phonon line, some type of filtering has to be performed. This can be achieved by selective excitation. Selectively excited PL (SPL) spectra were taken by adjusting the dye laser excitation wavelength to one of the known PLE peaks (see Sec. III B) and then recording the PL. As an example, we show in Fig. 7 the phonon structures accompanying the d_1 [Fig. 7(b)] and b_1 [Fig. 7(c)] no-phonon lines in the E_A spectrum of sample *A*. For comparison we have in-

TABLE I. No-phonon lines of the E_A spectrum of sample *A*. The position of the lines is given in the second and third columns and the seventh and eighth columns. The polarization with respect to the crystal *c* axis is given in columns five and ten. The fourth and ninth columns indicate the type of temperature behavior. *L* and *H* stand for low and high, respectively, and indicate whether a particular line is more intense at low or high temperature. The *b*, *c*, and *d* groups contain the strongest lines in the E_A spectrum and are also the first to be affected severely by annealing. They anneal out at around 750 °C.

Label	Position (Å)	Position (eV)	*L*/*H*	Polarization	Label	Position (Å)	Position (eV)	*L*/*H*	Polarization
a_1	4415.8	2.8069	*L*	$\overline{E}\perp\overline{c}$	f_3	4296.4	2.8850	*H*	$\overline{E}\perp\overline{c}$
a_2	4400.2	2.8169	*H*	$\overline{E}\perp\overline{c}$	f_4	4293.0	2.8872	*H*	$\overline{E}\perp\overline{c}$
b_1	4370.0	2.8364	*H*	$\overline{E}\perp\overline{c}$	g_1	4302.0	2.8812	*L*	$\overline{E}\|\overline{c}$
b_2	4356.2	2.8453	*H*	$\overline{E}\|\overline{c}$	g_2	4292.0	2.8879	*H*	$\overline{E}\perp\overline{c}$
c_1	4351.2	2.8486	*L*	$\overline{E}\|\overline{c}$	h_1	4298.2	2.8837	*L*	$\overline{E}\perp\overline{c}$
c_2	4344.6	2.8529	*H*	$\overline{E}\perp\overline{c}$	h_2	4286.2	2.8918	*H*	$\overline{E}\perp\overline{c}$
c_3	4341.6	2.8549	*H*	both	i_1	4283.4	2.8937	*L*	$\overline{E}\perp\overline{c}$
c_4	4340.0	2.8560	*H*	$\overline{E}\perp\overline{c}$	i_2	4272.4	2.9012	*H*	$\overline{E}\perp\overline{c}$
d_1	4347.0	2.8514	*L*	$\overline{E}\perp\overline{c}$	j_1	4277.6	2.8976	*L*	$\overline{E}\perp\overline{c}$
d_2	4335.6	2.8589	*H*	$\overline{E}\perp\overline{c}$	j_2	4270.6	2.9024	*H*	$\overline{E}\perp\overline{c}$
d_3	4334.2	2.8598	*H*	$\overline{E}\perp\overline{c}$	k_1	4276.2	2.8986	*L*	$\overline{E}\perp\overline{c}$
d_4	4330.6	2.8622	*H*	$\overline{E}\perp\overline{c}$	k_2	4268.4	2.9039	*H*	$\overline{E}\perp\overline{c}$
e_1	4326.8	2.8647	*L*	both	k_3	4264.6	2.9065	*H*	$\overline{E}\perp\overline{c}$
e_2	4314.8	2.8726	*H*	$\overline{E}\perp\overline{c}$	k_4	4263.4	2.9073	*H*	$\overline{E}\perp\overline{c}$
e_3	4308.6	2.8768	*H*	$\overline{E}\perp\overline{c}$	l_1	4274.4	2.8998	*L*	$\overline{E}\perp\overline{c}$
f_1	4310.4	2.8756	*L*	$\overline{E}\perp\overline{c}$	l_2	4262.4	2.9080	*H*	$\overline{E}\perp\overline{c}$
f_2	4300.0	2.8825	*H*	$\overline{E}\perp\overline{c}$	l_3	4261.4	2.9086	*H*	$\overline{E}\perp\overline{c}$

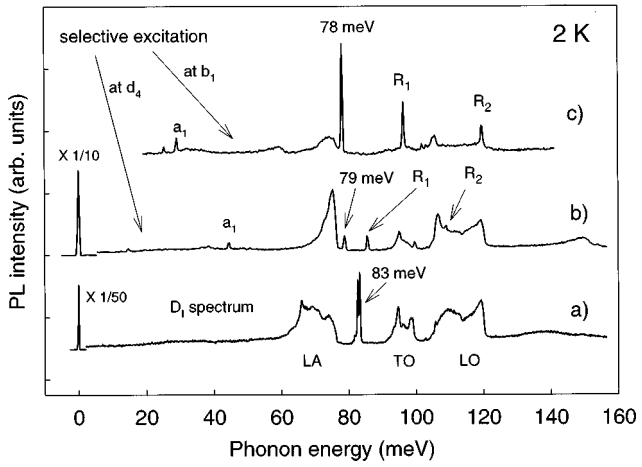

FIG. 7. The phonon structures accompanying (b) the d_1 no-phonon line and (c) the b_1 no-phonon line. For comparison we have included in (a) the low-temperature D_{I} PL spectrum in 4*H*-SiC consisting of the L_1 no-phonon line and the accompanying phonon structure. The spectra were recorded at 2 K. In the case of the d_1 spectrum, excitation at the d_4 no-phonon line position was used to feed the d_1 PL, but for the b_1 spectrum we excited directly at the b_1 no-phonon line. The lines denoted R_1 and R_2 in (b) and (c) are the folded TO and LO Raman modes of 4*H*-SiC at 96.2 and 119 meV from the laser line.

cluded the D_{I} PL spectrum in 4*H*-SiC [Fig. 7(a)] consisting of the L_1 no-phonon line and the accompanying phonon structure. The spectra were recorded at 2 K. In the case of the d_1 spectrum, excitation at the d_4 no-phonon line position was used to feed the d_1 PL, but for the b_1 spectrum we excited directly at the b_1 no-phonon line position. The sharp line at 78 meV below the b_1 line shows up strongly when selectively exciting at the b_1 line, but disappears when shifting slightly the excitation energy away from the b_1 line position. The line also has a similar temperature dependence to the b_1 line. This shows that it is a phonon replica of the b_1 line and not an independent no-phonon line. As the detection wavelength lies close to the excitation wavelength in these experiments, the spectra are influenced by Raman modes. The Raman peaks are easily identified by their shift and approximately constant intensity when shifting the excitation wavelength from the PLE peaks. The lines denoted R_1 and R_2 in Figs. 7(b) and 7(c) are the folded transverse optical and longitudinal optical Raman modes of 4*H*-SiC at approximately 96.2 and 119 meV from the laser line, respectively.

The main differences between the three spectra in Fig. 7 are the following. First, the sharp gap modes have different energies and different intensities relative to the broad structures. Second, the low-energy part of the longitudinal acoustic band observed in the case of D_{I} is absent in both the d_1 and b_1 spectra. Selective excitation was also carried out for the c_1 spectrum. Its phonon structure is very similar to that of the d_1 line.

Although the spectra in Figs. 7(b) and 7(c) are selectively excited, small traces of the a_1 line can be seen in both of them. This may be due to phonon-assisted excitation, or energy transfer between the different defects. The high-energy no-phonon lines of the E_A spectrum are much less intense than the low-energy ones, so this type of effect becomes more pronounced when attempting to selectively excite those lines. Thus, SPL spectra of the high-energy lines e_1, f_1, etc. include a considerable amount of PL belonging to the low-energy lines such as b_1, c_1, and d_1. Filtering by SPL is therefore not good in this case. The overall phonon structure of the E_A PL spectrum does not change much with temperature. This suggests that the phonon structure accompanying the high-temperature lines of each group is similar to that of the respective low-temperature line.

IV. DISCUSSION

From our results it is neither possible to determine which defects are responsible for the E_A PL spectrum nor to unambiguously identify the type of transitions involved. However, it is possible to eliminate certain possibilities and to suggest likely candidates.

In low-doped samples, the no-phonon lines of the E_A spectrum are symmetric and have half-widths less than 1 meV at temperatures as high as 60 K. For a transition involving a free carrier, the line form is determined by Maxwell-Boltzmann statistics and the half-width is expected to be approximately kT, where k is the Boltzmann constant and T is the temperature. This gives a half-width of $\sim$5 meV at 60 K. We conclude that the lines of the E_A spectrum do not involve free carriers, but are bound-state-to-bound-state transitions. The shape of the spectrum is not characteristic of a donor-acceptor pair emission. This leaves us with bound exciton recombination as the most likely alternative. Measurements of the decay times of the strongest E_A no-phonon lines at 2 K show that the lifetimes are on the order of 100 μsec.[19] This is much larger than for excitons bound at common donors and acceptors in SiC (see Ref. 20) and implies the absence of a competing Auger recombination. The rather large binding energy ($\sim$350–450 meV) indicates binding by short-range forces to isoelectronic centers according to experience with other semiconductors.[21] The ground state of this type of exciton often splits due to exchange coupling between the electron and the hole. Transitions from the lowest-energy state are usually dipole forbidden whereas those from the higher-energy states are dipole allowed. This can explain qualitatively both the temperature dependence and the PLE spectra of the lines in the E_A spectrum. Based on the above arguments, we suggest that the E_A spectrum is due to bound exciton recombination at several isoelectronic centers.

We cannot say much about the nature of the binding centers. In 4*H*-SiC there are two inequivalent substitutional sites. In most cases, the different substitutional sites are clearly reflected in the PL, as their spectra are shifted relative to each other. In 4*H*-SiC the number of spectra is therefore usually two for this type of defects. Examples are the N_C and Ti_{Si} bound exciton spectra. Therefore, if the E_A spectrum were due to single substitutional defects, we would, *a priori*, expect the line groups to come in pairs with similar characteristics. This, however, does not seem to be the case. Thus, it may be that the centers are not single defects, but some sort of complexes. Another possibility is that one of the two types of substitutional sites for some reason does not bind excitons.

We have not found any evidence supporting the involvement of impurities in the centers responsible for the E_A spectrum. The PL lines observed in Al or N doped substrates (see

Fig. 3) are also observed strongly in undoped CVD layers, although the impurity concentration in that case is orders of magnitude lower than in the doped samples. The effect of the doping on the spectrum is to enhance some of the no-phonon lines relative to the other no-phonon lines. This may be due to impurities, either at substitutional or interstitial sites, forming nonradiative complexes preferably with certain of the E_A centers and thereby rendering them inactive for PL.

The strong *b*, *c*, and *d* line groups of the E_A spectrum are the first to be affected severely by annealing. They all disappear abruptly at around 750 °C. From ODMR, EPR, and positron annihilation studies on different polytypes of SiC it has been observed that one of the main annealing stages of V_{Si}-related defects is between 700 and 800 °C.[2,3,12,22,23] This temperature may correspond to the migration temperature of the silicon vacancy.[2] In view of this, it is likely that the *b*, *c*, and *d* defects, which are responsible for the strongest lines in the E_A spectrum, are related to silicon vacancies.

V. SUMMARY

We have investigated the polarization, temperature dependence, and excitation properties of a PL spectrum, here called E_A, appearing after room-temperature electron irradiation of 4*H*-SiC. The spectrum consists of several sharp no-phonon lines accompanied by a broad phonon-assisted structure. Among the samples investigated were epitaxial layers of low residual doping and highly doped substrates. When the irradiation dose is high, the doping can affect the relative intensities of the different lines in the spectrum. Annealing at around 750 °C induces an abrupt change in the spectrum, whereas annealing at lower temperatures only causes minor changes. Further annealing steps occur at temperatures above 750 °C, eventually leading to the dominance of the strong D_I spectrum. Up to 40 no-phonon lines can be resolved in the E_A spectrum. All the no-phonon lines appear within the span of approximately 100 meV (2.8–2.9 eV). By PLE spectroscopy we are able to establish the relationship between most of the different lines. The lines come in groups of two to four lines. The general characteristics of the line groups suggest that they are due to bound exciton recombination at isoelectronic defect centers.

ACKNOWLEDGMENTS

Support for this work was provided by the Swedish Council for Engineering Sciences (TFR), the Swedish Foundation for Strategic Research (SSF), and ABB Corporate Research.

*Electronic address: tryeg@ifm.liu.se

[1] G. L. Harris, in *Properties of Silicon Carbide*, edited by G. L. Harris (INSPEC, London, 1995), p. 153.

[2] H. Itoh, A. Kawasuso, T. Oshmima, M. Yoshikawa, I. Nashiyama, S. Tanigawa, S. Misawa, H. Okumura, and S. Yoshida, Phys. Status Solidi A **162**, 173 (1997).

[3] J. Schneider and K. Maier, Physica B **185**, 199 (1993).

[4] T. Wimbauer, D. Volm, B. K. Meyer, A. Hofstätter, and A. Scharman, in *Proceedings of the 23rd International Conference on the Physics of Semiconductors*, edited by M. Scheffler and R. Zimmermann (World Scientific, Singapore, 1996), p. 2645.

[5] L. A. Balona and J. H. N. Loubster, J. Phys. C **3**, 2344 (1970).

[6] W. J. Choyke, Inst. Phys. Conf. Ser. **31**, 58 (1977).

[7] W. J. Choyke, in *The Physics and Chemistry of Carbides, Nitrides and Borides*, Vol. 185 of *NATO Advanced Study Institute Series E: Applied Sciences*, edited by Robert Freer (Kluwer Academic, Dordrecht, 1990), p. 563.

[8] L. Patrick and W. J. Choyke, Phys. Rev. B **5**, 3253 (1972).

[9] V. S. Vavilov, Yu. A. Vodakov, A. I. Ivanov, E. N. Mokhov, A. D. Roenkov, M. V. Chukichev, and R. G. Verenchikova, Sov. Phys. Semicond. **25**, 460 (1991).

[10] H. Itoh, M. Yoshikawa, I. Nashiyama, H. Okumura, S. Misakawa, and S. Yoshida, J. Appl. Phys. **77**, 837 (1995).

[11] N. T. Son, E. Sörman, M. Singh, W. M. Chen, C. Hallin, O. Kordina, B. Monemar, J. L. Lindström, and E. Janzén, Diamond Relat. Mater. **6**, 1378 (1997).

[12] E. Sörman, W. M. Chen, N. T. Son, C. Hallin, J. L. Lindström, B. Monemar, and E. Janzén, in *Proceedings of the 7th International Conference on Silicon Carbide, III-Nitrides and Related Materials, Stockholm, 1997*, edited by G. Pensl, H. Morkoç, B. Monemar, and E. Janzén [Mater. Sci. Forum **264-268**, 473 (1998)].

[13] N. T. Son (private communication).

[14] N. T. Son, E. Sörman, W. M. Chen, M. Singh, C. Hallin, O. Kordina, B. Monemar, E. Janzén, and J. L. Lindström, J. Appl. Phys. **79**, 3784 (1996).

[15] E. Sörman, N. T. Son, W. M. Chen, J. L. Lindström, O. Kordina, and E. Janzén, in *Proceedings of the 23rd International Conference on the Physics of Semiconductors* (Ref. 4), p. 2649.

[16] E. Sörman, N. T. Son, W. M. Chen, J. L. Lindström, and E. Janzén, in *Proceedings of the 19th International Conference on Defects in Semiconductors, Portugal, 1997*, edited by G. Davies and M. H. Nazaré [Mater. Sci. Forum **258-263**, 685 (1997)].

[17] I. G. Ivanov, A. Henry, U. Lindefelt, C. Persson, T. Egilsson, O. Kordina, C. Hallin, B. Monemar, and E. Janzén, in *Proceedings of the 23rd International Conference on the Physics of Semiconductors* (Ref. 4), p. 233.

[18] T. Egilsson, P. Bergman, I. G. Ivanov, A. Henry, and E. Janzén, Phys. Rev. B **59**, 1956 (1999).

[19] The lifetime measurements were made by Dr. Peder Bergman at Linköping University. The experimental conditions were the same as those described in Ref. 18.

[20] J. P. Bergman, O. Kordina, and E. Janzén, Phys. Status Solidi A **162**, 65 (1997).

[21] P. J. Dean and D. C. Herbert, in *Excitons*, edited by K. Cho, Topics in Current Physics Vol. 14 (Springer-Verlag, Berlin, 1979), p. 55.

[22] A. Kawasuso, H. Itoh, D. Cha, and S. Okada, in *Proceedings of the 7th International Conference on Silicon Carbide, III-Nitrides and Related Materials, Stockholm, 1997* (Ref. 12), p. 611.

[23] D. Cha, H. Itoh, N. Morishita, A. Kawasuso, T. Ohshima, Y. Watanabe, J. Ko, K. Lee, and I. Nashiyama, in *Proceedings of the 7th International Conference on Silicon Carbide, III-Nitrides and Related Materials, Stockholm, 1997* (Ref. 12), p. 615.